Dynamics of Photon Phase and Information Entropy for a Two-State Molecular System Interacting with Amplitude- and Phase-Squeezed Fields

ARTICLE *in* THE JOURNAL OF PHYSICAL CHEMISTRY A · JULY 1999

Impact Factor: 2.69 · DOI: 10.1021/jp991059z

2 AUTHORS, INCLUDING:

Masayoshi Nakano
Osaka University
337 PUBLICATIONS **4,781** CITATIONS

SEE PROFILE

Dynamics of Photon Phase and Information Entropy for a Two-State Molecular System Interacting with Amplitude- and Phase-Squeezed Fields

Masayoshi Nakano* and Kizashi Yamaguchi

Department of Chemistry, Graduate School of Science, Osaka University, Toyonaka, Osaka 560-0043, Japan

Received: March 26, 1999; In Final Form: May 21, 1999

From the viewpoints of photon-phase and information-entropy dynamics, we investigate the dynamical behavior of initially one-mode amplitude- and phase-squeezed photon fields interacting with a two-state molecular system. A peculiar behavior of these systems is known to be the collapses and revivals of Rabi oscillation of the molecular population. As shown in previous studies, significant differences are observed in the amplitude and the period of the collapse−revival behavior for these fields. These differences are found to be well-described by the dynamical behavior of the photon phase (the Pegg−Barnett phase and the quasiprobability (*Q* function) distributions). The features of these photon-phase dynamics are also found to provide significant influence on the time evolution of the information entropy of the molecule, which characterizes the degree of the entanglement between the molecule and the field.

1. Introduction

Great interest has been developed in the studies on the dynamics of molecular/atomic system interacting with the quantum field since the quantum field can provide various attracting influences on the dynamics, i.e., collapse, quiescence, and revival behavior,[1−6] which cannot be caused by conventional classical laser fields. Such dynamics is investigated using the Jaynes−Cummings (JC) model.[1−6] Mostly in this model, the two-state approximation to the atom system and the rotating-wave approximation (RWA) to the external photon field are used. It is well-known that these approximations work well and can provide analytical solutions in the case of simple atom systems interacting with near or resonant photon fields. Most of these studies have focused on the quantum mechanical nature of photon dynamics. On the other hand, there have been few studies on the interactions among molecules and quantized photon fields from the viewpoint of molecular science. In such studies, we need more general molecular models composed of an arbitrary number of states and the non-RWA scheme, which can treat external fields with arbitrary frequencies. In previous studies,[7−9] therefore, we performed a numerically exact treatment method of such dynamics, which is referred to as electron−photon field dynamics (EPFD), and elucidated the relations among molecular properties and the dynamics of coherent photon fields.

The phase information on the off-diagonal density matrices is known to be useful for understanding these dynamics. Recently, considerable progress in the study of the photon-phase properties of a radiation field has been made by Pegg and Barnett.[10−12] They introduced a set of formalisms defining a Hermitian phase operator, which allows us to calculate the phase distribution and various phase properties. On the other hand, the method based on a quasiprobability distribution, e.g., the *Q* function,[13] is widely used due to its less abstract and more pictorial description of radiation fields. These quantities are also considered to be useful for our understanding of the quantum dynamics of matter−field coupled systems. Actually, Meng and Chai[14] studied the photon-phase dynamics of an atom−coherent field coupled system in the JC model with the RWA, and Eiselt and Risken[15] elucidated the features of phase dynamics using the *Q* function distributions in the JC model with cavity damping. They found that the collapse and revival behavior in Rabi oscillation of the atomic population corresponds to the splitting and colliding processes of the peaks of the *Q* function distribution mutually counterrotating in the complex plane and found that the Pegg−Barnett (PB) phase distribution also exhibits similar splitting and colliding behavior in the phase space. In previous studies,[7−9] we elucidated the photon-phase dynamics for three- and four-state molecular model systems interacting with EPFD and found that the features of splitting and colliding processes of the phase distribution remarkably depend on the number of molecular states, molecular transition quantities (transition energies and properties), and the detuning of the external field. These results suggest that the photon-phase dynamics involves richer information on the time evolution of molecule−photon coupled systems than the population dynamics.

It is also well-known that the features of quantum dynamics for the JC models are found to remarkably depend on the quantum statistics of external fields. In particular, great effort has been devoted to the investigation of a squeezed field,[16−18] which has remarkable nonclassical features and is applicable in quantum communication and quantum nondemolition detection. The behavior of the atomic population for a squeezed field has been well-discussed by Milburn[19] and Satyanarayana et al.[20] They showed that a collapse time (see section 3.1) depends on the direction of the squeezing; for certain squeezed states the behavior of atomic population is similar to that for a chaotic field.[19] Further for a strongly squeezed field the behavior shows echoes after each revival, a phenomenon known as ringing revivals.[20] However, the behavior of photon-phase dynamics has not been elucidated for the squeezed field cases. In our previous study,[21] we investigated the features of photon-phase dynamics for an amplitude-squeezed field (with reduced amplitude fluctuations) interacting with a two-state molecule and elucidated some significant differences in the phase dynamics between the amplitude-squeezed and the coherent fields. Since the feature of dynamics for squeezed fields is known to be

10.1021/jp991059z CCC: $18.00
Published on Web 07/14/1999

sensitive to the squeezing angle,[19] we here consider another interesting squeezed field, i.e., the phase-squeezed field (with reduced phase fluctuations), in addition to the amplitude-squeezed and the coherent fields. These fields are assumed to possess the same average photon number. The Q function distribution and phase properties obtained by the PB phase operator are investigated for these fields. The simplest molecular model, i.e., a two-state model, is employed since we focus on the variation in the molecule−photon phase dynamics for the different quantum statistics of the initial fields. Another useful quantity characterizing quantum dynamics is the information entropy.[6,22−24] In general, the molecule−field coupled system evolves into an entangled state, where the molecule and the field subsystems separately are in mixed states. Since the features of such entanglement are well-described by the entropy of the subsystem, we analyze the features of the information entropy of the molecule (molecular entropy). The dynamical behavior of photon phases and molecular entropies for these squeezed and chaotic fields are discussed in connection with the dynamics of their molecular populations.

2. Methodology

In this section, a Hamiltonian for a molecule−photon coupled system and the calculation procedure of EPFD are presented. We also briefly explain the calculation method of molecular entropy and show how various photon-phase properties are calculated using the PB phase operator and the Q function.

2.1. Hamiltonian for a Molecule−Photon Field Coupled System. The Hamiltonian describing a molecular model with M states (M, integer) in a one-mode quantized field is constructed from H_{mol}, the Hamiltonian of the unperturbed molecule system; H_{field}, the Hamiltonian of the one-mode photon field; and H_{int}, the interaction Hamiltonian:

$$H = H_{\mathrm{mol}} + H_{\mathrm{field}} + H_{\mathrm{int}} \tag{1}$$

In the multipolar formalism under the dipole approximation, each part of the above Hamiltonian is expressed in the second-quantized representation as[7−9]

$$H_{\mathrm{mol}} = \sum_{i=1}^{M} E_i a_i^{+} a_i \tag{2}$$

$$H_{\mathrm{field}} = (n + {}^1/_2)\hbar\omega b^{+} b \tag{3}$$

$$H_{\mathrm{int}} = K \sum_{i,j=1}^{M} d_{ij} a_i^{+} a_j (b + b^{+}) \tag{4}$$

where

$$K = \left(\frac{\hbar\omega}{2\epsilon_0 V}\right)^{1/2} \tag{5}$$

In eq 2, E_i represents the energy of molecular state i and a_i^{+} and a_i are respectively the creation and annihilation operators for the quantized electron field in the ith energy state. In eq 3, n and ω indicate the photon number and the frequency of the one-mode photon field considered here, respectively, and b^{+} and b are the creation and annihilation operators for the one-mode photon field. d_{ij} is the matrix element of the molecular dipole moment operator in the direction of the polarization of the one-mode photon field. In eq 5, V is the volume of the cavity containing the one-mode photon field, and it is fixed to 10^7 Å^3 in this study.

The matrix elements of the above Hamiltonian are obtained using a double Hilbert space spanned by the molecular states $\{|i\rangle\}$ ($i = 1, 2, ..., M$) and the photon number states $\{|n\rangle\}$ ($n = 0, 1, 2, ..., \infty$). Namely, the double Hilbert space basis consists of the states $|i;n\rangle$ ($\equiv |i\rangle \otimes |n\rangle$). The matrix elements of the Hamiltonian, H_{mol}, H_{field}, and H_{int}, are expressed as follows.[7]

$$\langle j;n|H_{\mathrm{mol}}|j';n'\rangle = \sum_{i=1}^{M} \delta_{jj'i}\delta_{nn'}E_i \tag{6}$$

$$\langle j;n|H_{\mathrm{field}}|j';n'\rangle = \left(n + \frac{1}{2}\right)\hbar\omega\delta_{jj'}\delta_{nn'} \tag{7}$$

$$\langle j;n|H_{\mathrm{int}}|j';n'\rangle = K \sum_{i,i'=1}^{M} d_{jj'}\delta_{ij}\delta_{i'j'}((n+1)^{1/2}\delta_{n,n'-1} + n^{1/2}\delta_{n,n'+1}) \tag{8}$$

2.2. Procedure of Electron−Photon Field Dynamics. Before explaining the procedure of the EPFD, the matrix elements of the time-evolution operator and the density matrix of the molecule−photon field system are provided. Using the eigenvalues $\{W(m)\}$ and eigenvectors $\{\chi(m)\}$ ($m = 0, 1, 2, ...$) of the Hamiltonian (eq 1),

$$H|\chi(m)\rangle = W(m)|\chi(m)\rangle \tag{9}$$

where $m = 0, 1, 2, ...$, corresponds to $(i;n) = (1;0), (1;1), (1;2), ...$, respectively. Since this Hamiltonian is a Hermitian matrix, the eigenvectors $\{\chi(m)\}$ construct a complete orthonormal set:

$$\sum_m |\chi(m)\rangle\langle\chi(m)| = 1 \tag{10}$$

$$\langle\chi(n)|\chi(m)\rangle = \delta_{n,m} \tag{11}$$

In general, the solutions to the time-dependent Schrödinger equation,

$$i\hbar\frac{\partial}{\partial t}|\Psi(t)\rangle = H|\Psi(t)\rangle \tag{12}$$

are represented as

$$|\Psi(t)\rangle = \sum_n \mathrm{e}^{-iW(n)(t-t_0)/\hbar}|\chi(n)\rangle \equiv U(t,t_0)|\Psi(t_0)\rangle \tag{13}$$

where $U(t,t_0)$ is the time-evolution operator, which transforms the state at the initial time t_0 into the state at time t. The initial state vector, $|\Psi(t_0)\rangle$, is expressed by

$$|\Psi(t_0)\rangle = \sum_n |\chi(n)\rangle \tag{14}$$

The matrix element of the time-evolution operator is represented by

$$\langle j;n|U(t,t_0)|j';n'\rangle \equiv U_{j,n;j',n'} = \sum_m \langle j;n|\chi(m)\rangle\langle\chi(m)|j';n'\rangle \mathrm{e}^{-iW(m)(t-t_0)/\hbar} \tag{15}$$

The observable properties of photons and molecules are

described by using the density matrix

$$\langle j;n|\rho(t)|j';n'\rangle \equiv \rho_{j,n;j',n'}(t) = \sum_{f,g}^{M} \sum_{m,m'} U_{j,n;f,m}(t,t_0)\, \rho_{f,m;g,m'}(t_0)\, U^{+}_{g,m';j',n'}(t,t_0) \quad (16)$$

The procedure of EPFD is described as follows. Firstly, we construct an initial density matrix ($\rho_{f,m;g,m'}(t_0)$), which can be separated into the product of a molecular density matrix ($\rho_{f,g}(t_0)$) and a photon density matrix ($\rho_{m,m'}(t_0)$), as follows:

$$\rho_{f,m;g,m'}(t_0) = \rho_{f,g}(t_0)\, \rho_{m,m'}(t_0) \quad (17)$$

The molecule is assumed to be in the ground state at the initial time. As the initial photon fields, two types of squeezed fields, i.e., an amplitude- and a phase-squeezed field, and a coherent field are considered. The one-mode coherent field $|\beta\rangle$ is generated as follows from the vacuum field $|0\rangle$ by operating displacement operator.

$$|\beta\rangle = \exp(\beta b^{+} - \beta^{*} b)|0\rangle \quad (18)$$

where β is the eigenvalue of photon-annihilation operator b. The probability distribution of finding n photons in the coherent field is a Poisson distribution, and its element of the photon field density matrix is represented by

$$\rho_{n,m}(t_0) = \frac{\langle \hat{n}\rangle^{(n+m)/2} e^{-\langle \hat{n}\rangle}}{(n!m!)^{1/2}} \quad (19)$$

where $\langle \hat{n}\rangle$ is the mean number of photons in the coherent field. On the other hand, the one-mode ideally squeezed field can be generated from the vacuum field $|0\rangle$ by operating squeezing and displacement operators:

$$|\beta,\xi\rangle = \exp(\beta b^{+} - \beta^{*} b)\, \exp[(\xi^{*}\hat{b}^{2} - \xi(\hat{b}^{+})^{2})/2]|0\rangle \quad (20)$$

and ξ can be expressed by $\xi = re^{i\phi}$ using real modulus r and argument ϕ. The r and $\phi/2$ represent squeezing intensity and direction, respectively. The direction of β is taken to be aligned with the $Re(\beta)$ axis in the complex β plane. The squeezed field is generated by a number of molecular optical processes including optical parametric oscillation and four-wave mixing. This field state exhibits the property that the variance of the quadrature operator $\hat{x}_1(\hat{x}_2)$ is less than the value $^1/_2$ for the vacuum and the coherent field states. From the Heisenberg uncertainty relation between $\hat{x}_1$ and $\hat{x}_2$, the variance of another quadrature operator $\hat{x}_2$ ($\hat{x}_1$) exceeds $^1/_2$. If $\phi = 0$ in eq 20, the squeezed field has phase uncertainty higher than that of a coherent field of the same average photon number and a narrower photon-number distribution. This is referred to as an amplitude-squeezed field. If $\phi = \pi$ in eq 20, the squeezed field has an amplitude uncertainty higher than that of a coherent field and a broader photon-number distribution. This is referred to as a phase-squeezed field. In this study, we consider these two types of squeezed fields ($\phi = 0$ and π) with $r = 0.5$ for example. The elements of the squeezed field density matrix are represented by

$$\rho_{n,m}(t_0) = \frac{1}{|\mu|(n!m!)^{1/2}} \left(\frac{\nu}{2\mu}\right)^{n/2} \left(\frac{\nu^{*}}{2\mu^{*}}\right)^{m/2} \exp(-|\beta'|^2) \times \exp\left(\frac{1}{2}\frac{\nu^{*}}{\mu}(\beta')^2 + \frac{1}{2}\frac{\nu}{\mu^{*}}(\beta')^2\right) H_n{}^{*}\left[\frac{\beta'}{(2\mu\nu)^{1/2}}\right] H_n\left[\frac{\beta'}{(2\mu\nu)^{1/2}}\right] \quad (21)$$

where $\mu = \cosh r$, $\nu = e^{i\phi}\sinh r$, $\beta' = \mu\beta + \nu\beta^{*}$, and H_n is the Hermite function. Secondly, the density matrix elements ($\rho_{j,n;j',n'}(t)$) at time t are calculated using eqs 16 and 17. Thirdly, the molecular and photon reduced density matrix elements are, respectively, obtained by

$$\rho_{\mathrm{mol}j,j'}(t) = \sum_{n} \rho_{j,n;j',n}(t) \quad (22)$$

$$\rho_{\mathrm{photon}n,n'}(t) = \sum_{j} \rho_{j,n;j,n'}(t) \quad (23)$$

Finally, various properties concerning the photons and the molecule are calculated using these density matrices.

2.3. Pegg−Barnett Phase Operator and a Quasiprobability Distribution Function (*Q* Function). The phase properties of a one-mode photon field have been investigated since the first approach by Dirac.[25] Particularly, after Pegg and Barnett introduced a Hermitian phase operator[10−12] which overcomes several difficulties concerning the Susskind and Glogower phase operator,[26] the phase properties of coherent fields interacting with a two-state atom or a collection of atoms have been investigated.[7−9,14,15] Another quantity characterizing photon-phase properties is the quasiprobability distribution, which is similar to a true probability distribution for the field amplitude. Namely, the moments of products $\hat{b}$ and $\hat{b}^{+}$ can be calculated by evaluating an integral weighted by the quasiprobability distribution.

In the Pegg and Barnett approach, all calculations concerning the phase properties are performed in an $(s + 1)$-dimensional space spanned by $s + 1$ orthonormal phase states, and the s value will be taken to be infinity after all the expectation values have been calculated. The $s + 1$ orthonormal phase states are defined by

$$|\phi_m\rangle = \exp\left(i\frac{2\pi}{s+1}mn\right)|\phi_0\rangle \quad (24)$$

where

$$|\phi_0\rangle = \frac{1}{(s+1)^{1/2}} \sum_{n=0}^{s} \exp(in\phi_0)|n\rangle \quad (25)$$

Here, $\phi_m = \phi_0 + 2\pi m/(s+1)$ ($m = 0, 1, 2, ..., s$), and ϕ_0 is an arbitrary real number. In this study, we adopt $\phi_0 = -s\pi/(s+1)$ to locate the initial phase of a one-mode coherent photon field on the origin ($\phi = 0$) of the phase axis defined in the region $-\pi \le \phi_m \le +\pi$. Pegg and Barnett defined the following Hermitian phase operator to provide an eigenvalue ϕ_m and an eigenstate $|\phi_m\rangle$.

$$\hat{\phi} = \sum_{m=0}^{s} \phi_m |\phi_m\rangle\langle\phi_m| \quad (26)$$

On the basis of this definition, we can calculate the expectation values of arbitrary continuous functions of the phase operator ($f(\hat{\phi})$). By using PB operator, the operator $f(\hat{\phi})$ can be defined as

$$f(\hat{\phi}) = f\Big(\sum_{m=0}^{s} \phi_m |\phi_m\rangle\langle\phi_m|\Big) = \sum_{m=0}^{s} f(\phi_m)|\phi_m\rangle\langle\phi_m| \quad (27)$$

The expectation values of $f(\hat{\phi})$ for arbitrary physical states $|\psi\rangle$

can be calculated by

$$\langle f(\hat{\phi})\rangle = \lim_{s\to\infty}\langle\psi|f(\hat{\phi})|\psi\rangle = \lim_{s\to\infty}\sum_{m=0}^{s} f(\phi_m)\,P(\phi_m) \quad (28)$$

where $P(\phi_m)$ is a phase distribution function, which represents the probability that the phase of a physical state $|\psi\rangle$ is ϕ_m. Using eqs 23−25, the phase distribution function can be expressed by

$$P(\phi_m) = \frac{1}{s+1}\sum_{n,n'=0}^{s} \exp[i(n-n')\phi_m]\rho_{\text{photon}n'n} \quad (29)$$

Using eqs 28 and 29, we calculate $P(\phi_m)$, $\langle\cos^2\hat{\phi}\rangle$, and $\Delta\cos^2\phi$ for some molecule−photon field coupled systems at time t. In the present numerical calculations, s is taken to be 400. It is noted that time t is taken as $2\pi m/\omega$ ($m = 0, 1, 2, ...$) to remove the phase (ωt) of the free field.

The Q function is defined by

$$Q(\beta,t) = \frac{1}{\pi}\langle\beta|\rho_{\text{photon}}(t)|\beta\rangle = \frac{1}{\pi}\mathrm{e}^{-|\beta|^2}\sum_{n,n'=1}\frac{(\beta^*)^{n-1}\beta^{n'-1}}{[(n-1)!(n'-1)!]^{1/2}}\rho_{\text{photon}n,n'}(t) \quad (30)$$

where $|\beta\rangle$ is a coherent state, β is its complex amplitude, and n is a photon number.

2.4. Molecular Entropy. The molecular entropy is calculated by

$$S_{\text{mol}} = -\text{Tr}(\rho_{\text{mol}}\ln\rho_{\text{mol}}) = -\sum_{i=1}^{M}\rho'_{\text{mol }ii}\ln(\rho'_{\text{mol }ii}) \quad (31)$$

where ρ'_{mol} is the diagonalized molecular reduced density matrix. For a pure state, $S_{\text{mol}} = 0$, while, for a mixed state, $S_{\text{mol}} = 1$. Namely, the time evolution of the molecular entropy reflects the time evolution of the degree of entanglement between the molecule and the field. The larger the entropy, the greater the entanglement.

3. Quantum Dynamics of a Two-State Molecular System Interacting with Initially One-Mode Squeezed Fields and a Coherent Field

We consider a two-state molecular system with energy intervals E_{21} ($\equiv E_2 - E_1$) = 37 800 cm^{-1} and the transition moments $d_{21} = 5$ D. The near-resonant frequency of an initially one-mode photon field is 37 750 cm^{-1}. The average photon number $\langle\hat{n}\rangle$ is fixed at 8. At the initial time, the molecule is assumed to be in the ground state. Figures 1 and 2 show the photon-number distributions (a), the time developments of the molecular ground-state populations (b), and the phase properties ($\langle\cos^2\hat{\phi}\rangle$ (c) and $\Delta\cos^2\phi$ (d)) of the external photon fields (Figure 1 for the amplitude-squeezed field and Figure 2 for the phase-squeezed field). The results of the coherent field are also shown as a reference in these figures.

3.1. Amplitude-Squeezed Field Case. As shown in Figure 1a, the amplitude-squeezed field exhibits a narrower (sub-Poissonian) photon-number distribution than that of the coherent field. This distribution feature can be easily understood by the phase−photon-number uncertainty. Since the phase-squeezed field hardly exhibits oscillatory photon-number distribution, we can say that this squeezing ($r = 0.5$) is not so strong.

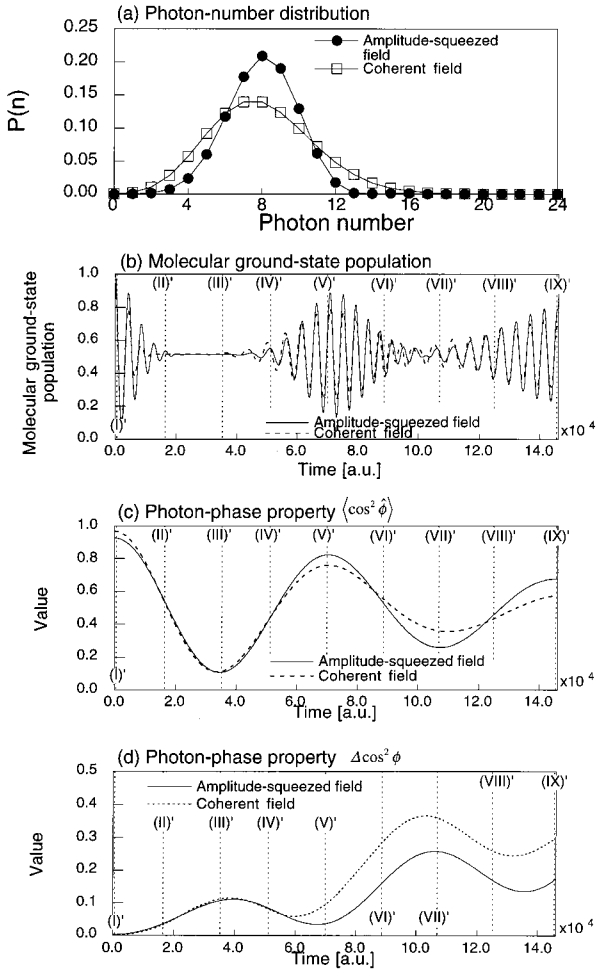

Figure 1. (a) Photon-number distribution for a coherent and an amplitude-squeezed field. (b) Molecular ground-state population changes and photon-phase properties ((c) $\langle\cos^2\hat{\phi}\rangle$ and (d) $\Delta\cos^2\phi$) for a system composed of a two-state molecular system (transition energy, E_{21} = 37 800 cm^{-1}; transition moment, $d_{21} = 5$ D) and a one-mode photon field. At the initial time, the molecule is assumed to be in the ground state, and the photon field is in one-mode amplitude-squeezed (r = 0.5, $\phi = 0$) (solid lines in b−d) and coherent (dotted lines in b−d) states ($\langle\hat{n}\rangle = 8$, ω = 37 750 cm^{-1} for both fields).

The molecular ground-state populations for the amplitude-squeezed and coherent fields (Figure 1b) exhibit damped oscillations, i.e., collapses, and amplified oscillations, i.e., revivals, in the early time region. At later times, these collapses and revivals are found to overlap with each other and to be difficult to divide clearly. The mechanism and the features of this behavior have been well-analyzed,[1−6] and then the collapse and revival behavior are found to originate in the dephasing and the rephasing among Rabi oscillations with slightly different frequencies, respectively. In comparison with the coherent field case (Figure 1b), the first collapse time (the time taken for the envelope to collapse to zero) for the amplitude-squeezed field is longer, while the first revival time (the time taken for the most complete revival of the initial population) coincides. Therefore, the first revival−collapse period for the amplitude-squeezed field case is found to be shorter than that for the coherent field case. For the amplitude-squeezed field case, the revival is shown to be narrower and the maximum amplitude of the oscillations is shown to be larger than that for the coherent field case. These features were firstly analyzed by Milburn.[19] It was shown that the revival time depends only on the initial

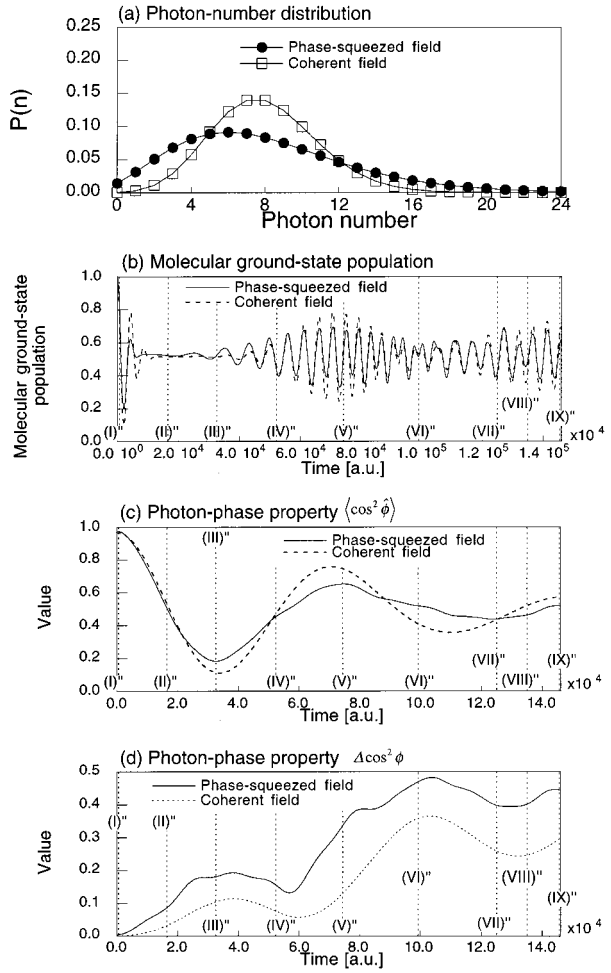

Figure 2. (a) Photon-number distribution for a coherent and a phase-squeezed field. (b) Molecular ground-state population changes and photon-phase properties ((c) $\langle \cos^2 \hat{\phi} \rangle$ and (d) $\Delta \cos^2 \phi$). At the initial time, the photon field is in one-mode phase-squeezed ($r = 0.5$, $\phi = \pi$) (solid lines in b−d) and coherent (dotted lines in b−d) states. See Figure 1 for further legends.

average photon number, while the collapse time depends not only on the initial average photon number but also its statistical nature through Δn ($\equiv \langle \hat{n}^2 \rangle - \langle \hat{n} \rangle^2$). In this study, such behavior is alternatively investigated using photon-phase properties.

For the photon-phase properties $\langle \cos^2 \hat{\phi} \rangle$ shown in Figure 1c, the damped oscillations are observed for the amplitude-squeezed and the coherent fields. At the initial time, $\langle \cos^2 \hat{\phi} \rangle$ for the coherent field is found to be nearly equal to 1, while that for the amplitude-squeezed field is found to be slightly smaller. This reflects the fact that, at the initial time, the amplitude-squeezed field has higher phase uncertainty than does the coherent field. It is also found that the amplitudes of the oscillations of $\langle \cos^2 \hat{\phi} \rangle$ for the amplitude-squeezed field are larger than those for the coherent field particularly at later times (IV)′−(IX)′. Further, as shown in Figure 1d, the $\Delta \cos^2 \phi$ for the amplitude-squeezed field is shown to slowly increase compared with that for the coherent field. These features indicate that the phase fluctuation for the coherent field rapidly increases compared with that for the amplitude-squeezed field. The distinct collapse−revival oscillations, with larger maximum amplitudes, for the amplitude-squeezed field are considered to be ascribed to a slower increase such as this in the phase fluctuation.

3.2. Phase-Squeezed Field Case. Contrary to the amplitude-squeezed field (Figure 1a), the phase-squeezed field exhibits a broader (super-Poissonian) photon-number distribution than that of the coherent field (see Figure 2a). This feature also can be understood by the phase−photon-number uncertainty. Since the phase-squeezed field hardly exhibits oscillatory photon-number distribution, this squeezing ($r = 0.5$) is not so strong for the phase-squeezed field.

The molecular ground-state population for the phase-squeezed field (Figure 2b) also exhibits collapses and revivals. Although the first revival time for the phase-squeezed field is shown to coincide with that for the coherent field, the first collapse time for the phase-squeezed field is shown to be shorter than that for the coherent field. The first revival−collapse period for the phase-squeezed field is found to be longer than that for the coherent field. Also, the maximum amplitude of its revival oscillations is found to be smaller than that for the coherent field. These features are contrary to those for the amplitude-squeezed field (see Figure 1). Such differences are understood by the fact that the revival time depends only on the initial average photon number ($\langle \hat{n} \rangle = 8$ in this study), while the collapse time depends not only on the initial average photon number but also on its statistical nature through Δn ($\equiv \langle \hat{n}^2 \rangle - \langle \hat{n} \rangle^2$)[19] ($\Delta n = 2.828$ for the coherent field, $\Delta n = 1.880$ for the amplitude-squeezed field, and $\Delta n = 4.658$ for the phase-squeezed field).

The damped oscillation of $\langle \cos^2 \hat{\phi} \rangle$ for the phase-squeezed field (Figure 2c) is shown to have smaller amplitudes than that for the coherent field. Further, as shown in Figure 2d, $\Delta \cos^2 \phi$ for the phase-squeezed field is shown to rapidly increase and to take larger values compared with that for the coherent field. In contrast to the amplitude-squeezed field case (see Figure 1), these features indicate that the phase fluctuations for the phase-squeezed field rapidly increase compared with that for the coherent field. Such behavior of the phase fluctuation leads to the obscure collapse−revival behavior for the phase-squeezed field (Figure 2b). In order to better elucidate these behaviors of photon-phase properties, we investigate the dynamics of the PB phase and the Q function distributions in the next section.

4. PB Phase and Q Function Distribution Dynamics of a Two-State Molecular System Interacting with Initially One-Mode Squeezed Fields and Coherent Field

The PB phase and Q function distributions (Figures 3 and 4 for the coherent field, Figures 5 and 6 for the amplitude-squeezed field, and Figures 7 and 8 for the phase-squeezed field) are given at each time (represented by (I)−(IX), (I)′−(IX)′, and (I)″−(IX)″). The (I)−(IX) represent the times for local maxima and local minima of $\langle \cos^2 \hat{\phi} \rangle$ (Figures 1c and 2c) and their intermediate times for the coherent field. The (I)′−(IX)′ and (I)″−(IX)″ represent the similar times (shown in Figures 1c and 2c) for the amplitude- and the phase-squeezed fields, respectively.

4.1. Amplitude-Squeezed Field Case. *4.1.1. PB Phase Distribution Dynamics.* As expected from the definition of amplitude squeezing, the phase distribution at time (I)′ of the amplitude-squeezed field (Figure 3((I)′) is shown to be broader than that of the coherent field (see Figure 3(I)). At the times (II) and (II)′ shown in Figures 3 and 5, a single peak at $\phi = 0$ is found to split into two peaks with asymmetric intensities. This feature is considered to originate in the differences in the absorption of photons. Namely, in the case of the external field frequency of 37 750 cm^{-1} ($< E_{21} = 37\,800$ cm^{-1}), a negative phase tends to bring the external field frequency close to the resonant frequency and thus to enhance the absorption of photons, while a positive phase tends to bring the external field frequency away from the resonant frequency and thus to reduce

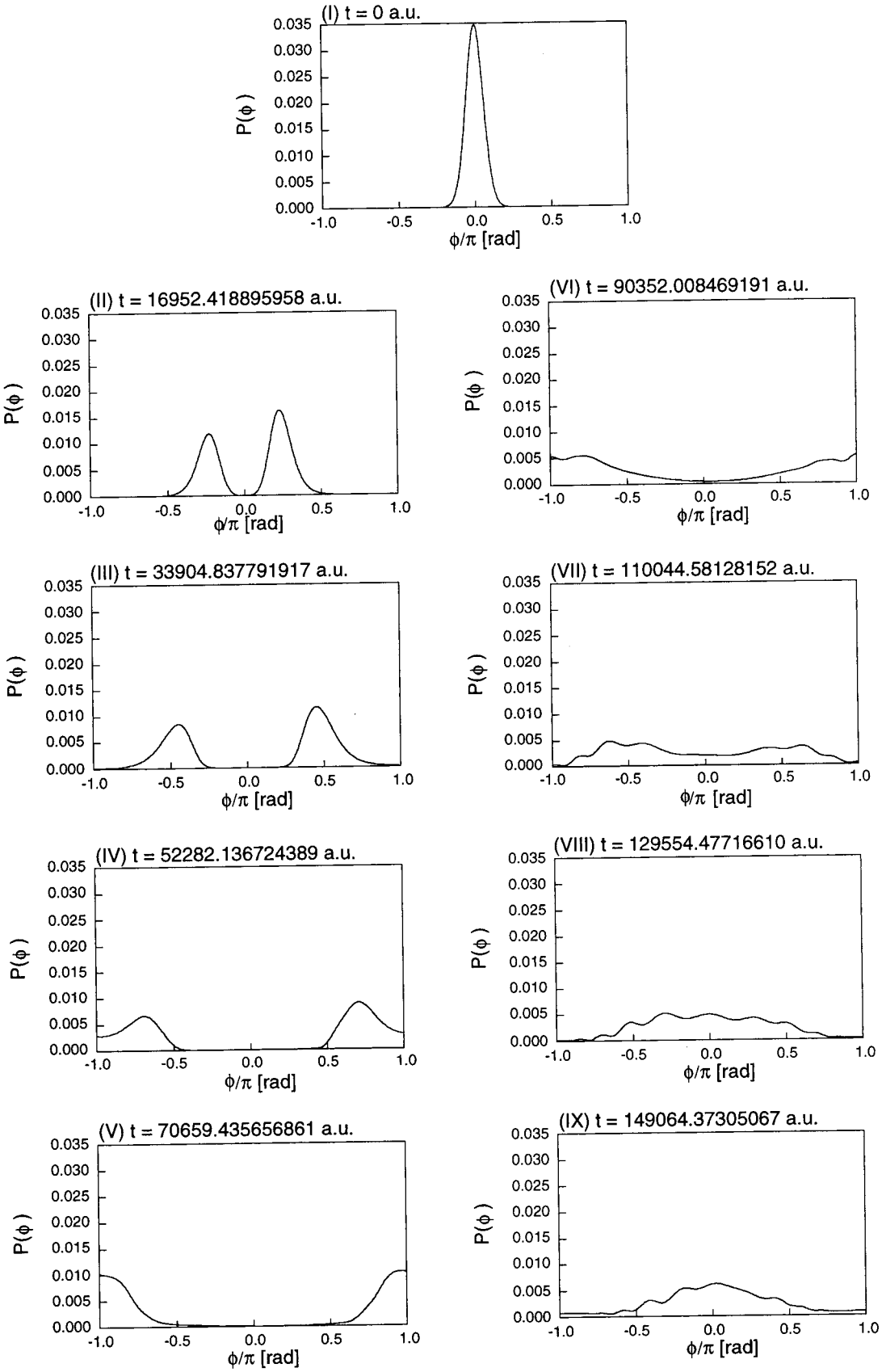

Figure 3. Pegg−Barnett phase distributions $P(\phi)$ at times (I)−(IX) (see section 4.1. 1) for the coherent field interacting with the two-state molecular system (see legends of Figure 1). The parameter s (given in eq 30) is taken to be 400.

the absorption of photons. This feature corresponds to the asymmetric photon-phase distribution: the peak intensity in the positive phase region is larger than that in the negative phase region. At the time (II)′ shown in Figure 5, the phase distribution at $\phi = 0$ for the amplitude-squeezed field is also found to slightly exist though that for the coherent field is found to be nearly equal to zero (see Figure 3(II)). This corresponds to the slower collapse behavior in the molecular ground-state popula-

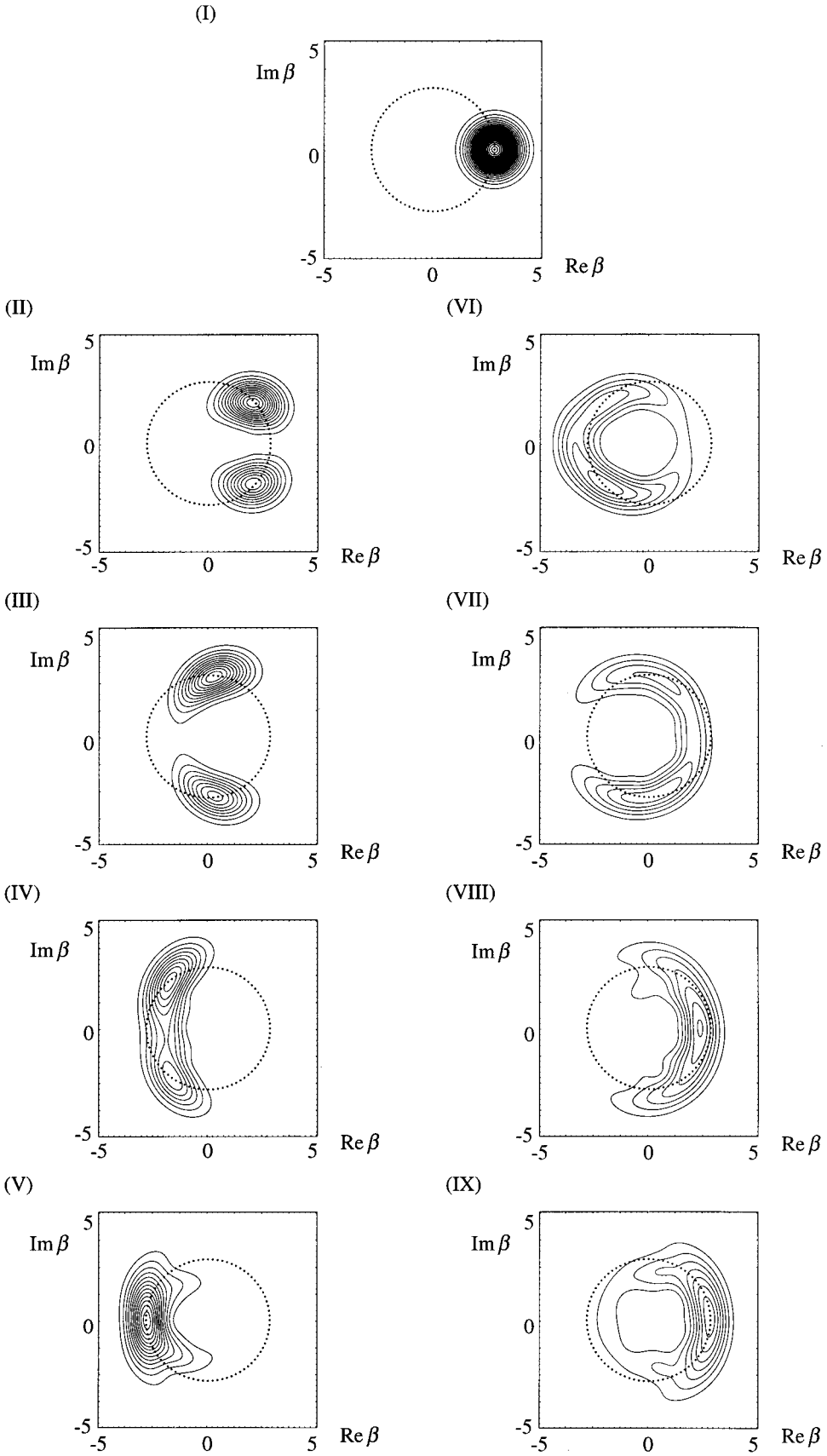

Figure 4. $Q(\beta,t)$ function distributions in the complex β plane for times (I)−(IX) (see section 4.1.2) for the coherent field interacting with the two-state molecular system (see Figure 1). The circle $|\beta| = \langle\hat{n}\rangle^{1/2}$ ($\langle\hat{n}\rangle$, average photon number of the initial photon field) is also dotted in the contour plots.

tion for the amplitude-squeezed field (see Figure 1b). At the time (III)′ for the amplitude-squeezed field (Figure 5), the distribution inside the split peaks is larger than that outside the split peaks, in contrast to the case of the coherent field (see

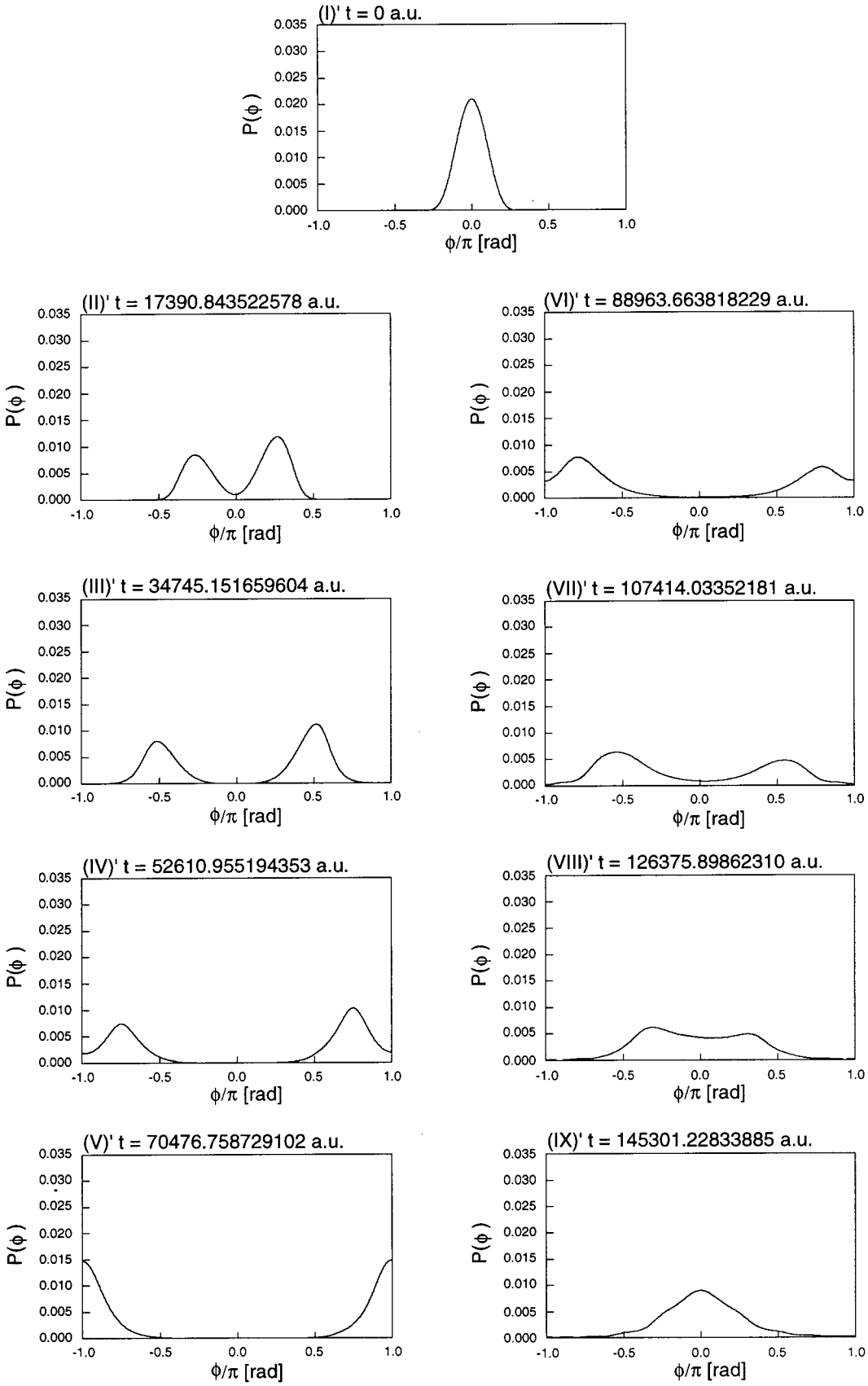

Figure 5. Pegg−Barnett phase distributions $P(\phi)$ at times (I)′−(IX)′ (shown in Figure 1) for the amplitude-squeezed field ($r = 0.5$, $\phi = 0$) interacting with the two-state molecular system. See Figure 3 for further legends.

Figure 3(III)). At the time (V)′ shown in Figure 5, the split peaks are shown to collide at $\phi = \pm\pi$. It is considered that the splitting process in the photon-phase distribution first causes the increase in the ability to destruct the coherence between the molecular ground and excited states and then causes the gradual decrease in that ability due to the large splitting of the photon phase (approaching $\phi = \pm\pi/2$). In contrast, the colliding process is considered to cause the gradual increase and successive decrease

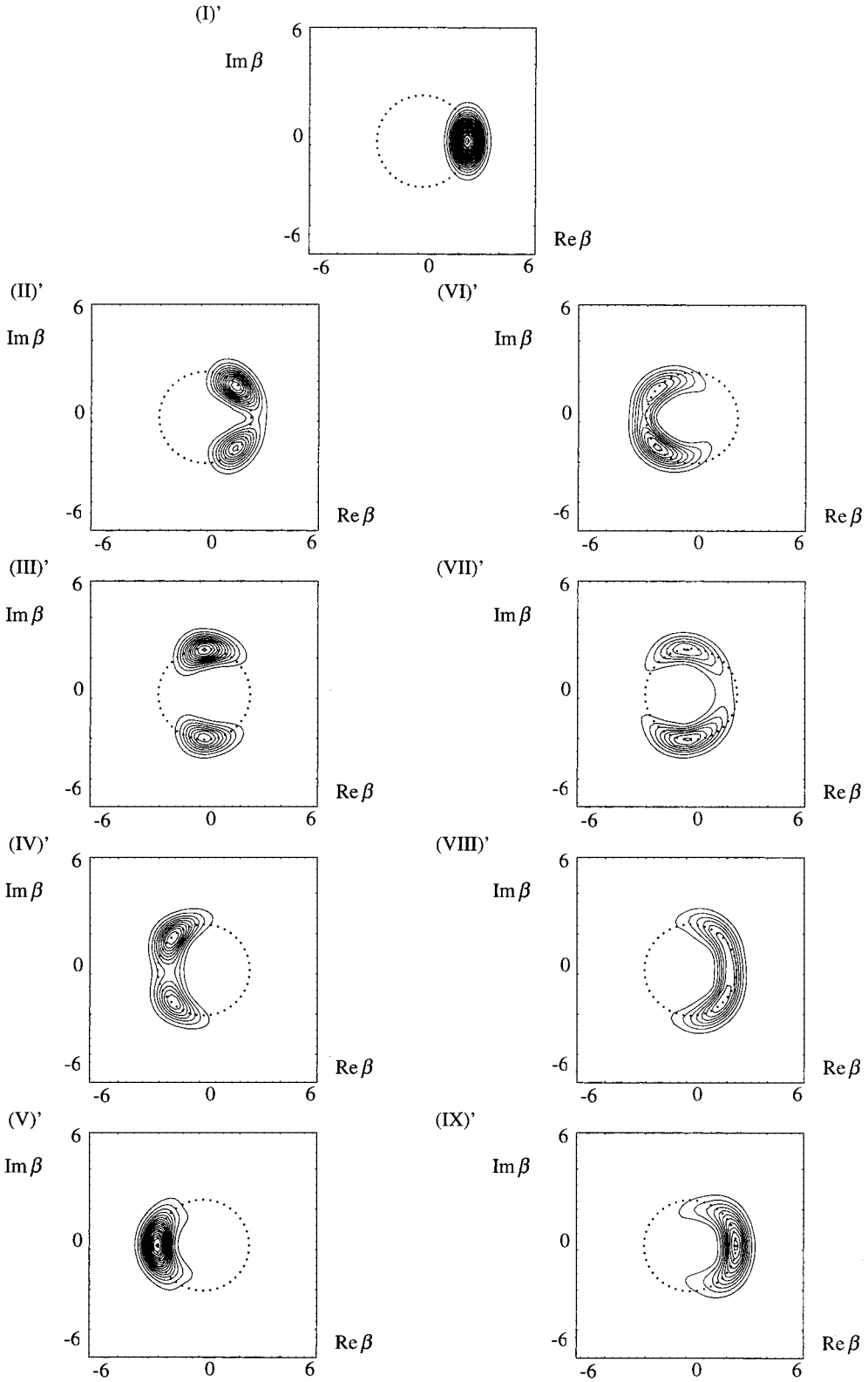

Figure 6. $Q(\beta,t)$ function distributions in the complex β plane for times (I)′−(IX)′ (shown in Figure 1) for the amplitude-squeezed field ($r = 0.5$, $\phi = 0$) interacting with the two-state molecular system. See Figure 4 for further legends.

in that ability. As seen from the damped oscillation of $\langle \cos^2 \hat{\phi} \rangle$ (Figure 1c), however, the splitting and colliding are not completely achieved, so that the increase and decrease changes in that ability are considered to become unclear as time proceeds. These splitting and colliding processes in the PB phase distribution are observed equally for the amplitude-squeezed and the coherent fields (see Figures 3 and 5).

In the early time region (I)′−(II)′ ((I)−(II)) (Figures 3 and 5), the PB phase distributions for the amplitude-squeezed field are shown to be broader than those for the coherent field, and then the splitting of the initial single peak for the amplitude-squeezed field becomes slower than that for the coherent field. This feature supports the delay of the first collapse of the molecular population for the amplitude-squeezed field (Figure 1b). As shown in the phase distributions at the later times (IV)−(IX) ((IV)′−(IX)′) (Figures 3 and 5), however, the phase

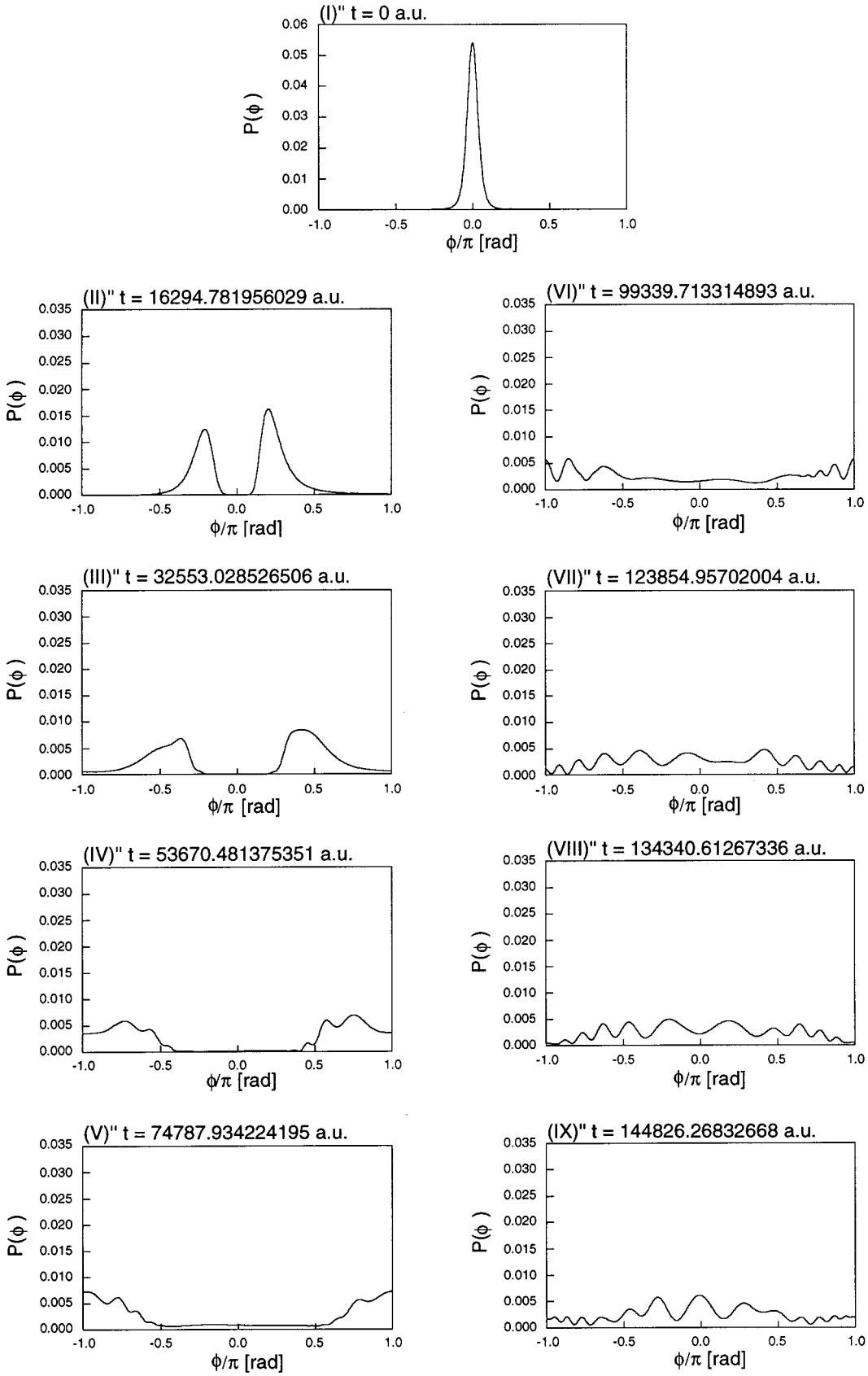

Figure 7. Pegg−Barnett phase distributions $P(\phi)$ at times (I)″−(IX)″ (shown in Figure 1) for the phase-squeezed field ($r = 0.5$, $\phi = \pi$) interacting with the two-state molecular system. See Figure 3 for further legends.

distribution peaks for the amplitude-squeezed field (Figure 5) become more distinct than those for the coherent field (Figure 3). This feature corresponds to the fact that more distinct collapse and revival behavior with larger amplitudes is observed at the later times (IV)′−(IX)′ for the amplitude-squeezed field (see Figure 1b).

4.1.2. Q Function Distribution Dynamics. The feature of phase dynamics observed in section. 4.1.1 is well-understood

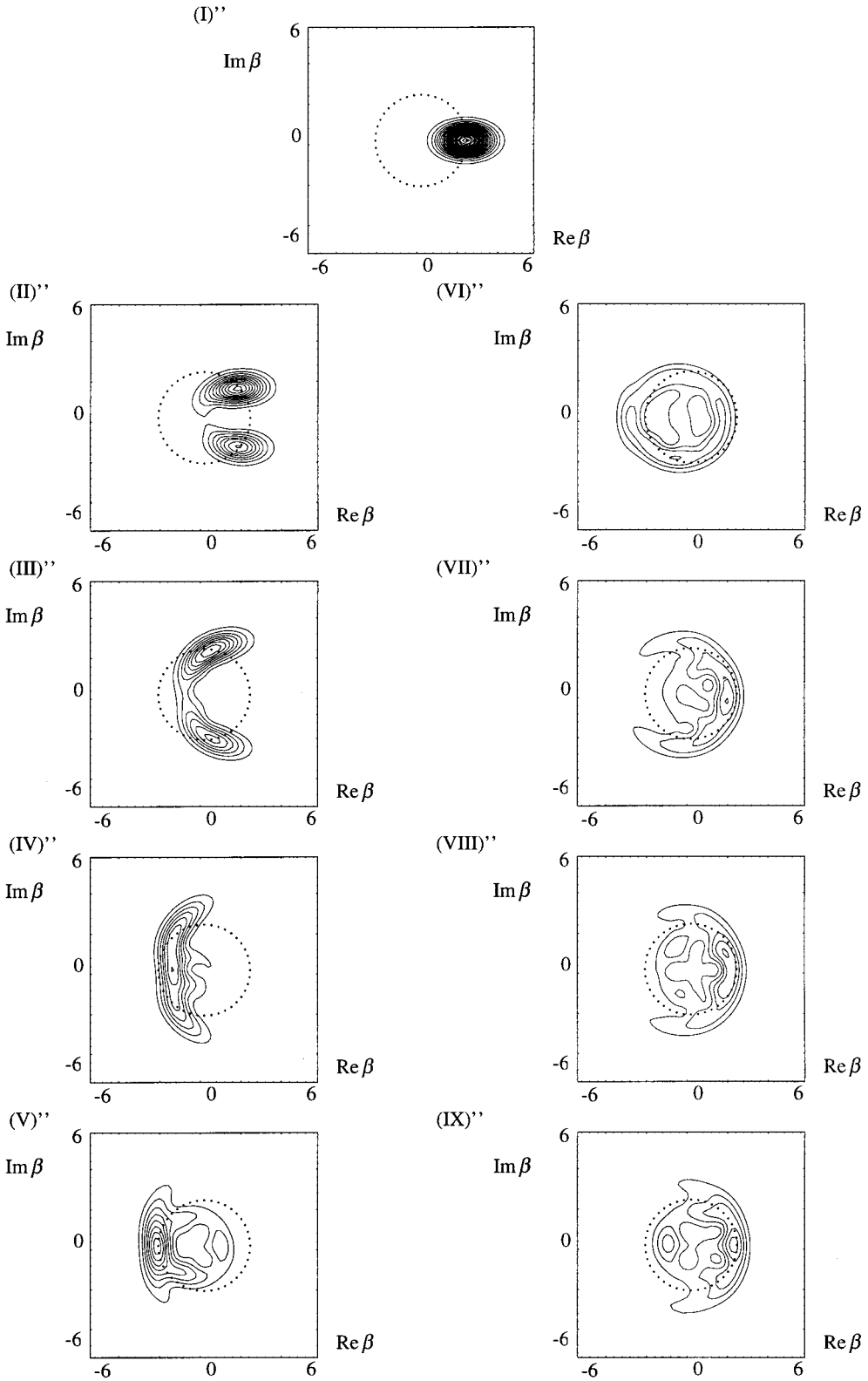

Figure 8. $Q(\beta,t)$ function distributions in the complex β plane for the times (I)″−(IX)″ (shown in Figure 2) for the phase-squeezed field ($r = 0.5$, $\phi = \pi$) interacting with the two-state molecular system. See Figure 4 for further legends.

by investigating the Q function distributions at the times (I)−(IX) ((I)′−(IX)′) (Figure 4 for the coherent field and Figure 6 for the amplitude-squeezed field). In contrast to the coherent field, the initial Q function is shown to provide an ellipse distribution centered around β_0 ($\equiv\langle\hat{n}\rangle^{1/2}$, $\langle\hat{n}\rangle = 8$) (see Figure 6((I)′).

Firstly, we investigate the common features of the Q function dynamics for the amplitude-squeezed and the coherent fields. As shown in Figures 4 and 6, a single peak at $\phi = 0$ is found to split into two peaks with asymmetric intensities and then counterrotate on the circle $|\beta| = \beta_0$ until they collide at $\phi = \pm\pi$. After this collision, they split again and collide at $\phi = 0$. It is found that these splitting and colliding processes repeat, though the distribution peaks are gradually broadened. The splitting of the single peak in the time region (I)−(III) ((I)′−(III)′) is found to correspond to the collapse behavior of the

molecular ground-state population. This feature supports the decrease in $\langle \cos^2 \hat{\phi} \rangle$ in the same time region (see Figure 1c). At the time (III) ((III)′), $\langle \cos^2 \hat{\phi} \rangle$ is found to be a minimum value since the split peaks on the complex plane are shown to be located at $\phi = +\pi/2$ and $-\pi/2$, respectively. In the next time region (III)−(V) ((III)′−(IV)′), the split peaks are shown to rotate in mutually opposite directions and then to collide at $\phi = \pm\pi$. This variation leads to the increase in $\langle \cos^2 \hat{\phi} \rangle$ in the time region (III)′−(V)′ ((III)−(V)) (see Figure 1c). Similar behavior of the *Q* function distribution and $\langle \cos^2 \hat{\phi} \rangle$ are observed in the time regions (V)−(VII) ((V)′−(VII)′) and (VII)−(IX) ((VII)′−(IX)′). Throughout these processes, the peaks are found to gradually decrease and to cause a broadening, which leads to the slowly oscillating increase in $\Delta \cos^2 \phi$ (see Figure 1c). This behavior is considered to be due to the uncertainty relation between a photon phase and a photon number.

Next, we elucidate the differences in the *Q* function distribution dynamics for the amplitude-squeezed and the coherent fields. In a comparison of Figure 4 (II) with Figure 6 ((II)′), the squeezing in the direction of the *Re*(β) axis is found to cause the delay of splitting of the initial distribution, the feature of which corresponds to those of the PB phase distributions shown in Figure 5 ((I)′ and (II)′). Since it was also found that for a larger photon number the *Q* function distribution needs a longer time to split,[15] the broader photon-number distribution for the coherent field (characterized by the distribution in the inner and outer regions of the circle $|\beta| = \beta_0$) leads to the enhancement of the range of the rotation speed of split peaks. Namely, in comparison with the coherent field, the range of the rotation speed of split peaks for the amplitude-squeezed field is considered to reduce, so that the split distributions for the amplitude-squeezed field become more distinct and sharper at the later times (IV)′−(IX)′. These features in phase distribution support the peculiar collapse−revival behavior for the amplitude-squeezed field: a longer first collapse time, a shorter revival−collapse period, and larger revival−collapse amplitudes.

4.2. Phase-Squeezed Field Case. *4.2.1. PB Phase Distribution Dynamics.* In contrast to the amplitude-squeezed field case (Figure 5), the phase distribution peak at the time (I)″ for the phase-squeezed field is shown to be sharper than that for the coherent field (see Figure 3 (I)). Similarly to the amplitude-squeezed field in section 4.1, the splitting and colliding behavior of the phase distribution peaks is observed. The relations among the phase distribution dynamics and the collapse−revival behavior of the molecular ground-state population are the same as those in the coherent field case (see section 4.1.1). The split phase peaks for the phase-squeezed field are shown to be lower and to have larger distributions in higher $|\phi|$ regions compared with the coherent field case (see Figures 3 ((III)−(IX)) and 7 ((III)″−(IX)″)). Such faster broadening of phase distribution peaks corresponds to the faster decrease in the ability to destruct the coherence between the molecular ground and excited states. This supports the obscure collapse and revival behavior with smaller amplitudes at the later times (II)″−(VI)″ for the phase-squeezed field (see Figure 2b).

4.2.2. Q Function Distribution Dynamics. In contrast to the coherent field (Figure 4), the initial distribution of the *Q* function is shown to provide an ellipse distribution centered around β_0 ($\equiv \langle \hat{n} \rangle^{1/2}$, $\langle \hat{n} \rangle = 8$) (see Figure 8 ((I)″).

The common features of *Q* function dynamics for the phase-squeezed and the coherent fields are the same as those discussed in our previous section 4.1.2. As shown in Figures 4 (II) and 8 (II)″), the splitting behavior of the *Q* function distribution for the phase-squeezed and the coherent fields is found to be similar to each other. In contrast to the amplitude-squeezed field (Figure 6), however, the squeezing in the direction of the *Im*(β) axis is found to decrease the phase uncertainty compared with the coherent field and thus causes the faster splitting of the initial *Q* function distribution. Also, contrary to the amplitude-squeezed field, the squeezed distributions in the inner and outer regions of the circle $|\beta| = \beta_0$ indicate the existence of the *Q* function distributions with faster and slower rotating speeds compared with the coherent field case. This is considered to cause the faster broadening and extending of the *Q* function distribution along the circle $|\beta| = \beta_0$, the feature of which corresponds to the dynamical behavior of the PB phase distribution shown in Figure 7. Consequently, such dynamical behavior of the phase distributions is found to support the faster collapse ((I)″−(II)″) and the longer revival−collapse period ((III)″−(VI)″) with smaller revival−collapse amplitudes shown in Figure 2b.

5. Molecular Entropy Dynamics

It is well-known that the molecular entropy for the coherent field starts from zero due to the initial pure state of the molecule, increases (with modulation at the Rabi oscillation), and then decreases during the collapse process. At the half-revival time during the collapse, the molecular entropy is known to take a local minimum, which means the molecule returns most closely to a pure state.[5] The momentarily created nearly-pure molecular state is a coherent superposition of the two energy state of the molecule, while the photon state is a macroscopic superposition (optical Schrödinger cat) state composed of the phase components $\phi = -\pi/2$ and $+\pi/2$.[15] These features are well-observed in the present coherent field shown in Figure 7a.

As shown in Figure 9, the molecular entropies of the present amplitude- and phase-squeezed fields are found to have features similar to those of the coherent field (Figure 9a), i.e., a decrease at the times (I)−(III) ((I)′−(III)′ and (I)″−(III)″) and an increase at the times (III)−(VII) ((III)′−(VII)′ and (III)″−(VII)″). However, the variation in amplitude of the molecular entropy for the amplitude-squeezed field (Figure 9b) is found to be larger than that for the coherent field, while that for the phase-squeezed field (Figure 9c) is found to be smaller than that for the coherent field. It is also found that the fine oscillations in molecular entropy of the amplitude-squeezed field (Figure 9b) are more remarkable than those of the phase-squeezed field. These features correspond well to those of the amplitudes for the ground-state populations for these fields and thus reflect the differences observed in the dynamics of the PB phase and the *Q* function distributions among the coherent, the amplitude-squeezed, and the phase-squeezed fields. Namely, the more remarkable splitting and colliding features in the phase distributions for the amplitude-squeezed field are considered to cause such distinct variation in the entropy dynamics compared with the phase-squeezed field.

6. Concluding Remarks

The present study elucidated the dynamics of a two-state molecular system interacting with amplitude- and phase-squeezed fields ($r = 0.5$). As observed in previous studies,[15] it was found for these squeezed fields that the splitting into two peaks and their colliding processes in the PB phase and the *Q* function distributions correspond to the collapse and revival behavior of the molecular population. It was also found that there are significant differences among the features of phase dynamics for the these squeezed fields and those for the coherent field. For the amplitude-squeezed field, there were found to be broader PB phase distributions in the early time region (I)′−

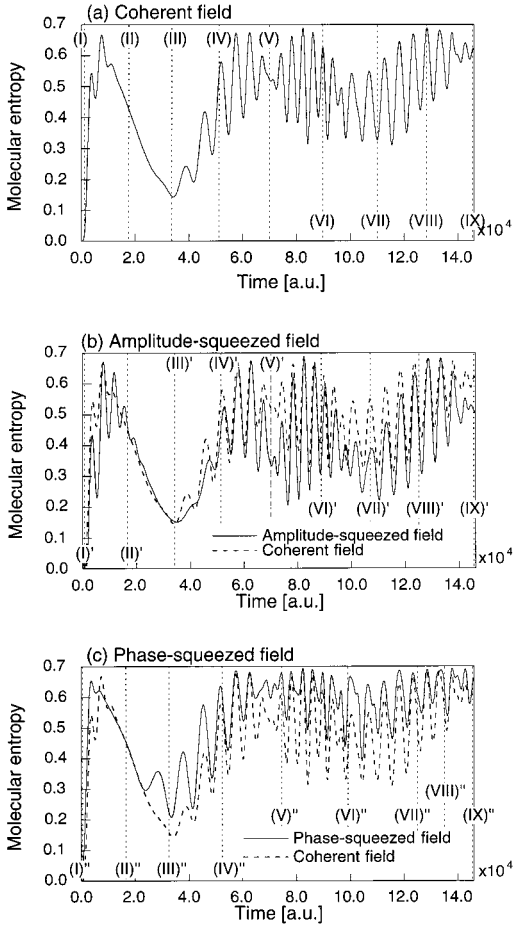

Figure 9. Time evolution of the molecular entropies for the (a) coherent, (b) amplitude-squeezed, and (c) phase-squeezed fields. The molecular entropy of the coherent field is also shown by a dotted line in b and c for comparison.

(II)′ and more distinct two split Q function distributions, which counterrotate on the circle $|\beta| = \beta_0$, in the later time region (IV)′−(IX)′. These features support the slower collapse behavior with larger amplitudes in the early time region (I)′−(II)′ and the more distinct collapse−revival behavior in the later time region (IV)′−(IX)′. On the other hand, for the phase-squeezed field, there were found to be a Q function distribution squeezed in the direction of $Im(\beta)$ at early times and more obscure two split Q function peaks distributed on more extended regions along the circle $|\beta| = \beta_0$ at later times. These features of phase dynamics support the faster collapse behavior in the early time region (I)″−(II)″ and the more obscure collapse−revival behavior with smaller amplitudes in the later time region (IV)″−(IX)″ for the phase-squeezed field. From the present results, in the case of the squeezing parameter $r = 0.5$, the collapse and revival behavior of the molecular population were shown to become obscure in the following order: the amplitude-squeezed field, the coherent field, and the phase-squeezed field. Such differences were found to be closely related to the differences in the phase distribution dynamics, largely affected by the quantum statistics of the initial fields.

Further, the features of the molecular entropy dynamics, which indicates the degree of the entanglement between the photon and the molecular states, are also found to indicate the differences among these fields. Namely, there are found to be more distinct variations in the molecular entropy for the amplitude-squeezed field than those for the phase-squeezed field. These features in the molecular entropy dynamics are also found to closely relate to those in the photon-phase (PB phase and Q function distributions) dynamics.

From the present study, the viewpoints of photon-phase and information-entropy dynamics are expected to be useful for providing the intuitive and pictorial understanding of the dynamics for more general molecular systems (composed of a larger number of states) interacting with various types of quantum fields.

Acknowledgment. This work was supported by a Grant-in-Aid for Scientific Research on Priority Areas (No. 10149101 and 11166239) from the Ministry of Education, Science, Sports and Culture, Japan, and a grant from the CASIO Science Promotion Foundation.

References and Notes

(1) Jaynes, E. T.; Cummings, F. W. *Proc. IEEE* **1963**, *51*, 100.
(2) Allen, L.; Eberly, J. H. *Optical Resonance and Two-Level Atoms*; Wiley: New York, 1975.
(3) Knight, P. L.; Milonni, P. W. *Phys. Rep.* **1980**, *66*, 21.
(4) Milonni, P. W.; Singh, S. *Adv. At., Mol., Opt. Phys.* **1990**, *28*, 75.
(5) Shore, B. W.; Knight, P. L. *J. Mod. Opt.* **1993**, *40*, 1195.
(6) Aravind, P. K.; Hirschfelder, J. O. *J. Phys. Chem.* **1984**, *88*, 4788.
(7) Nakano, M.; Yamaguchi, K. *Chem. Phys.*, submitted for publication.
(8) Nakano, M.; Yamaguchi, K. *Chem. Phys. Lett.* **1998**, *295*, 317.
(9) Nakano, M.; Yamaguchi, K. *Chem. Phys. Lett.* **1998**, *295*, 328.
(10) Pegg, D. T.; Barnett, S. M. *Europhys. Lett.* **1988**, *6*, 483.
(11) Barnett, S. M.; Pegg, D. T. *J. Mod. Opt.* **1989**, *36*, 7.
(12) Pegg, D. T.; Barnett, S. M. *Phys. Rev. A* **1989**, *39*, 1665.
(13) Glauber, R. J. In *Quantum Optics and Electronics*; DeWitt, C., Blandin, A., Cohen-Tannoudji, C., Eds.; Gordon and Breach: Reading, U.K., 1965.
(14) Meng, H. X.; Chai, C. L. *Phys. Rev. A* **1992**, *45*, 2131.
(15) Eiselt, J.; Risken, H. *Phys. Rev. A* **1991**, *43*, 346.
(16) Stoler, D. *Phys. Rev. D* **1970**, *1*, 3217; **1971**, *4*, 1925.
(17) Yuen, H. P. *Phys. Rev. A* **1976**, *13*, 2226.
(18) Walls, D. W. *Nature* **1983**, *306*, 141.
(19) Milburn, G. *Opt. Acta* **1984**, *31*, 671.
(20) Satyanarayana, M. V.; Rice, P.; Vyas, R.; Carmichael, H. J. *J. Opt. Soc. Am. B* **1989**, *6*, 228.
(21) Nakano, M.; Yamaguchi, K. *Chem. Phys. Lett.* **1999**, *304*, 241.
(22) Wehrl, A. *Rev. Mod. Phys.* **1978**, *50*, 221.
(23) Phoenix, D. S. J.; Knight, P. L. *Ann. Phys.* **1988**, *186*, 381.
(24) Glauber, R. J. *Phys. Rev.* **1963**, *130*, 2529.
(25) Dirac, P. A. M. *Proc. R. Soc. London, Ser. A* **1927**, *114*, 243.
(26) Susskind, L.; Glogower, J. *Physics* **1964**, *1*, 49.